# Comparative Study of Flow Stress Modeling of Zircaloy-4 Sheets Manufactured from Different Routes

Kanthi Limbadri[a], Kurra Suresh[b,*], Swadesh Kumar Singh[c,d]

[a]MLR Institute of Technology, Hyderabad 500 043, India

[b]BITS Pilani, Hyderabad Campus, 500 078, India

[c]GokarajuRangaraju Institute of Engineering and Technology, Hyderabad 500090, India

[d]Institute for Sustainable Industries & Livable Cities, Victoria University, P.O. Box 14428, Melbourne, VIC 8001, Australia

Zircaloy-4 is proven to be an excellent structural material in the nuclear industry. In the present work, three types of zircaloy-4 sheet materials are subjected to tensile tests at strain rates of $0.001s^{-1}$, $0.005s^{-1}$, $0.01s^{-1}$, and at four different temperatures of 298K(room temperature), 348K, 423K, and 498K.The tensile stress-strain data has been used to model the flow stress using three different constitutive models, namely the Johnson-Cook (JC) model, modified Zerilli-Armstrong (m-ZA), and modified Arrhenius (m-Arr) model. The models' prediction capability for all the materials is compared using the Coefficient of correlation (R), average absolute error (Δ), and the number of constants to be determined. It has resulted that the m-Arr model has high goodness of fit with a maximum R-value is 0.9950,and the minimum Δ is1.1132% for Low Oxygen Sheet (LOS) material. It is alsoa suitable model for the other two zircaloy-4 materials, even though more constants are to be evaluated.

**Keywords:** Zircaloy-4, Johnson-Cook model, Modified Zerilli-Armstrong, Modified Arrhenius, Coefficient of correlation

## 1 Introduction

Over the years, the Zircaloy-4 has been widely used structural material in nuclear industries due to its corrosion resistance at high temperatures, good creep strength, and low thermal neutron absorption cross-section, and moderate mechanical properties[1]. This material is mainly used as cladding tube and spacer grids due to their texture dependent tensile flow behavior. For such an important material, it is crucial to develop constitutive equations used in finite element code for simulation of material deformation during processes.

Many works have been reported the constitutive models developed for different materials. Modified Johnson Cook model (m-JC), m-ZA, m-Arr and KHL models have been developed for Inconel 625 superalloy to analyze the effect of strain rate and temperature on flow stress; it has been concluded that the m-Arris more suitable[2]. The arrhenius-type equation has been used to predict the flow stress behaviour of Aluminium alloy 7A04 when it is subjected to isothermal compression test at elevated

temperatures. It has resulted in good agreement with experimental data[3].

The Prediction of flow stress for uniaxial isothermal and dynamic compression tests at a range of 673K to 1373K has been done with m-ZA, Cowper Symonds (CS), m-JC, Arr, KHL, and The m-JC has been noted as better suitable model[4]. Different types of Arrhenius-type constitutive models have been used for predicting tensile behavior of 17-PH stainless steel sheet, and accurate prediction has resulted through multi-strain modified models[5]. In a comparison study on prediction accuracy of m-ZA and m-JC for isothermal deformation of Aluminium 5083 + SiC composite, the m-ZA has been identified as a better suitable model[6]. JC, m-JC, FB, KHL, and Mechanical Threshold Stress (MTS) constitutive equations have been developed for Ti-6Al-4V alloy at low strain rates and elevated temperatures. Their prediction capabilities also have been compared with statistical parameters[7,8]. The tensile behavior of near alpha titanium alloys is also modeled by JC constitutive equation[9]. M-FB, JC, and Arr models have predicted flow stress behavior of friction welding of GH4169 superalloy. The experimental stress data has been in good agreement with the predicted stress through

―――――――――
*Corresponding author

(E-mail: ksuresh@hyderabad.bits-pilani.ac.in)

Arr.[10]. The experimental compressive stress of Al-Zn-Mg-Cu aluminum alloy at elevated temperatures has been compared with the predicted stress through the Arrhenius type equation, and it has resulted ina high Coefficient of correlation (R) of 0.993[11]. The hyperbolic-sine Arrhenius equation has been used to predict the hot compression stress of two different titanium alloys. The model's prediction capacity has also been improved by the reduced gradient refinement method[12]. Similarly, JC, m-ZA, m-Arr, also developed for the austenitic stainless steel 316 at the temperature range of 323-623K, and the strain rate range is 0.05-0.3[13]. Maraging steel M300 compressive stress behavior is also modeled using the Arrhenius equation[14]. Furthermore, the hot deformation behavior of 7055 Aluminium alloy is analyzed by phenomenological models: JC, modified Fields-Backofen (m-FB), Arrhenius (Arr). It was concluded that Arr predicts well due to taking into consideration of strain rate – temperature combined effect[15]. Besides, the JC model and ZA models have been integrated to better predict flow stress for Ti-6Al-4V alloy at high strain rate and elevated temperatures[16]. FB, Fields-Backofen-Zhang (FBZ), and modified Field-Backofen-Zhang (m-FBZ) have been used for predicting the isothermal tensile flow stress of alpha-Ti tubes. Among the three, m-FBZ model prediction is very accurate, with an R-value of 0.9873[17]. JC, m-JC models have been employed to predict the flow stress of Al7075 at elevated temperatures, and due to the modification of temperature term in JC, the m-JC has given accurate prediction[18].

In relation to Zircaloy-4, a modified Johnson-Cook model has been developed. This model has been used for the simulation of pilgering process. The results have been shown that predicted flow stress is greater than the experimental flow stress[19]. A macro constitutive model was developed for reactivity-initiated accident (RIA) loading conditions by Sauxet *et al*[20,21]. Hill 48 yield criteria analysed material anisotropy of Zircaloy-4 with a combination of isotropic hardening model[22]. None of the work, especially for the Zircaloy-4, explained the suitable model for stress prediction.

In the present work, phenomenological constitutive equations such as JC, m-Arr and physical-based equation, m-ZA, are caliburated for three different types of Zircaloy-4 materials. The isothermal uniaxial tensile test data was used to determine the constant of the models, and subsequently, the predictability of

these models for the three Zircaloy-4 materials are compared using statistical parameters such as Coefficient of correlation(R) and average absolute error (Δ).

## 2 Materials and Methods

In the present work, three types of Zircaloy-4 materials are used for making tensile specimens, namely: Slab Route Sheet (SRS), Tube Route Sheet (TRS), and Low Oxygen Sheet (LOS). The SRS is a rolled and annealed sheet. The TRS is manufactured from pilgering method. The LOS sheet is rolled sheet and comparatively it has less oxygen content.

The sub size tensile specimens of ASTM standard E8/E8M-11 were used in the experiments and it is shown in our previously published work[1]. The samples were cut from raw sheet materials by wire-cut electro-discharge machining method for high accuracy. The tensile tests were conducted as per the ASTM E8 standard on the Electra-50 BISS servo-electric universal testing machine of 50 kN capacity at three different strain rates ($0.001s^{-1}$, $0.005s^{-1,}$ and $0.01s^{-1}$) and four temperatures (Room temperature (298K), 348K, 423K, and 498K) and the experimental setup is shown in our previously published work [1]. Once the tensile tests were conducted, the load vs. displacement data was taken as the raw data and converted into true stress and true strain data. The true stress and true strain data is converted into true stress vs. true plastic strain by deleting the elastic component of the data. During the experiments, the constant strain rates are obtained by varying the cross-head velocity in an exponential manner with the help of a feedback control system. The cross-head velocity is as given in Eq. 1.

$$v = \dot{\varepsilon} L exp(\dot{\varepsilon} t) \qquad \qquad ... (1)$$

where $v, L$ and $t$ are cross-head velocity, gauge length of the specimen, and time respectively

## 3 Results and Discussion

The constitutive models trace out the flow stress behavior of materials. In the present work, two phenomenological, JC and m-Arr, and one physical based, ZA, are developed. Even though the models are developed for all three materials, the graphs are plotted using the data of the LOS material as a matter of explanation.

### 3.1 Johnson-Cook (JC) model

According to the original JC model[23], the flow stress can be expressed as in the form of the Eq. (2).

$$\sigma = (A + B\varepsilon^n)(1 + Cln\dot{\varepsilon}^*)(1 - T^{*m}) \qquad \dots (2)$$

Here the $(A + B\varepsilon^n), (1 + Cln\dot{\varepsilon}^*)$ and $(1 - T^{*m})$ terms represent isothermal hardening, strain rate hardening, and thermal softening, respectively. $\sigma$ stands for flow stress, $\varepsilon$ stands for true plastic strain, $A$ is the yield stress at reference temperature and strain rate, $B$ is the Coefficient of strain hardening, $n$ is the strain hardening exponent, $C$ is the Coefficient of strain rate hardening, $m$ stands for thermal softening exponent. $\dot{\varepsilon}^* = \dot{\varepsilon}/\dot{\varepsilon}_o$, where $\dot{\varepsilon}$ is strain rate and $\dot{\varepsilon}_o$ is reference strain rate. $T^*$ is homologous temperature as given in Eq.(3).

$$T^* = \frac{T - T_{ref}}{T_m - T_{ref}} \qquad \dots (3)$$

where $T$ is absolute temperature, $T_{ref}$ is reference temperature, $T_m$ is melting temperature and always holds the $T \geq T_{ref}$. Generally, the $T_{ref}$ is taken as the lowest temperature from the experimental values. Since the JC model accounts for the isolation from each of the phenomena for isothermal hardening, strain rate hardening, and thermal softening, the expression can be written as the multiplication of the three terms. The different materials constants of the JC model are systematically determined by considering other conditions as follows.

### 3.1.1 Condition 1: At reference temperature and reference strain rate

At reference temperature and reference strain rate, both the thermal softening and strain rate hardening terms becomes equal to 1. Hence, the modified Eq. 1 is expressed in Eq. (4)

$$\sigma = A + B\varepsilon^n \qquad \dots (4)$$

The value of $A$ is yield stress at the reference temperature of 298K and reference strain rate of $0.001s^{-1}$. Now, by plotting the line between $\ln(\sigma - A)$ and $\ln(\varepsilon)$ at reference strain rate and reference temperature, the '$n$' and '$B$' constants are calculated from slope and intercepts.

### 3.1.2 Condition 2: At reference temperature and fixed strain

At reference temperature, the isothermal softening term equals one, and the Eq.1 reduces to Eq.5.

$$\sigma = (A + B\varepsilon^n)(1 + Cln\dot{\varepsilon}^*) \qquad \dots (5)$$

Since it is a fixed strain condition, for each value of strain, a line is plotted between $\frac{\sigma}{A + B\varepsilon^n} - 1$ and $ln\dot{\varepsilon}^*$, from which the slope '$C$' value is obtained.

### 3.1.3 Condition 3: At reference strain rate and fixed strain

At reference strain rate, the strain rate hardening contribution in Eq.1 becomes equal to 1; therefore, the Eq.1 is reduced to Eq. (6).

$$\sigma = (A + B\varepsilon^n)(1 - T^{*m}) \qquad \dots (6)$$

It is also a fixed strain condition. Therefore, for each value of $\varepsilon$, a line between $\ln\left[1 - \frac{\sigma}{A + B\varepsilon^n}\right]$ and $\ln(T^*)$ is plotted to get the slope '$m$' value. Here again, for each value of $\varepsilon$ there is an m value.

### 3.1.4 Condition 4: Optimization of C and m values

Since there are numbers of C and m values obtained, the least-squares method can determine the optimized values. This approach works on constrained optimization by minimization of average absolute error $(\Delta)$ between experimental stress $(\sigma_{exp})$ and predicted stress $(\sigma_p)$ as given in Eq. (7).

$$\Delta = \frac{1}{N} \sum_{i=1}^{i=N} \left| \frac{\sigma_{exp}^i - \sigma_p^i}{\sigma_{exp}^i} \right| \times 100 \qquad \dots (7)$$

where $N$ is total number of data points, $\sigma_{exp}$ is experimental stress, $\sigma_p$ is predicted stress by using each couple of $C$ and $m$ values corresponding to their strain values. The constitutive equation's prediction capacity can also be obtained by calculating the Coefficient of correlation (R). The coefficient correlation is a statistical parameter obtained from the linear relation between experimental stress values and predicted stress values. The mathematical expression of the $R$-value is given in Eq. (8).

$$R = \frac{\sum_{i=1}^{i=N}(\sigma_{exp}^i - \bar{\sigma}_{exp})(\sigma_p^i - \bar{\sigma}_p)}{\sqrt{\sum_{i=1}^{i=N}(\sigma_{exp}^i - \bar{\sigma}_{exp})^2 \sum_{i=1}^{i=N}(\sigma_p^i - \bar{\sigma}_p)^2}} \qquad \dots (8)$$

where $\bar{\sigma}_{exp}$ and $\bar{\sigma}_p$ are mean values of experimental and predicted stresses, respectively. Since the $R$ values have a tendency to be biased, it is not necessary that the higher value of the $R$ refer better performance of the model in prediction. This $\Delta$ gives unbiased value due to the involvement of term by term defining the error[28]. Hence, both R and $\Delta$ values must be considered in the analysis of predictability of the constitutive model.

All the determined values of A, B, n, C, and m are listed in Table 1. By substituting all the determined constants, the JC model for LOS can be written as in Eq. (9).

$$\sigma = (337.86 + 461.74\varepsilon^{0.3600})(1 - 0.0367ln\dot{\varepsilon}^*)(1 - T^{*0.9794}) - \qquad \dots (9)$$

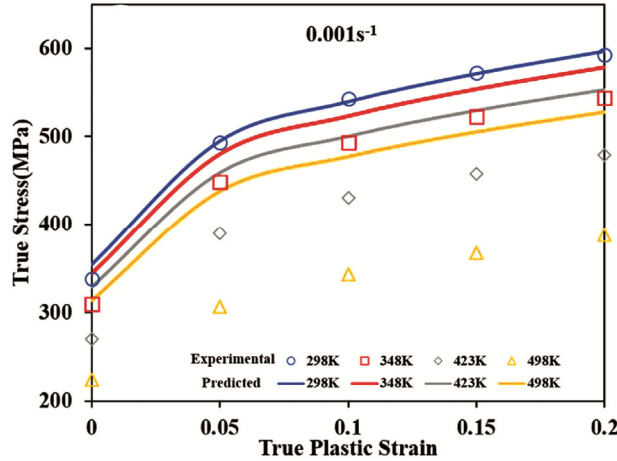| Table 1 — Deterimined constants of JC model | | | | |
|---|---|---|---|---|
| | A (MPa) | B (MPa) | C | m | n |
| LOS | 337.86 | 461.74 | -0.0367 | 0.9794 | 0.36 |
| SRS | 353.75 | 415.05 | 0.0131 | 0.6098 | 0.4025 |
| TRS | 375.26 | 468.72 | -0.01 | 0.8964 | 0.4519 |



Fig. 1 — Validation of predicted stress with experimental stress data using JC model at 0.001s$^{-1}$ strain rate.

Using the Eq.9, the stress data is predicted and compared with experimental data, as shown in Fig. 1.

**3.2 Modified Zerilli-Armstrong (m-ZA) model**

According to the original Zerilli-Armstrong model[23],the flow stress is expressed in Eq. (10).

$$\sigma = A_0 + A_1\varepsilon^n \exp\left(T(A_2 ln\dot{\varepsilon} - A_3)\right) \quad \text{... (10)}$$

where $\sigma$ is flow stress, $A_0$ is the thermal component of yield stress, $A_1, A_2, A_3$ and n are material constants, $\varepsilon$ is the true plastic strain, $T$ is the absolute temperature and $\dot{\varepsilon}$ is true plastic strain rate.

The original Zerilli-Armstrong model has two components, thermal and athermal. The thermal component is $A_1\varepsilon^n \exp\left(T(A_2 ln\dot{\varepsilon} - A_3)\right)$ and the athermal component is $A_0$. While the thermal component depends on experimental temperature, the athermal component depends on the material's grain size during deformation. The thermal component can be inferred in Fig. 1, Fig. 2, and Fig. 3, where the flow stress decreases with an increase in temperature. In the modified Zerilli-Armstrong (m-ZA) model, the athermal component was neglected, and the modified equation is expressed in Eq. (11).

$$\sigma = (C_1 + C_2\varepsilon^n)e^{[-(C_3 + C_4\varepsilon)T^* + (C_5 + C_6 T^*)ln\dot{\varepsilon}^*]} \quad \text{... (11)}$$

where $\sigma$ stands for flow stress,$C_1$ is taken as yield stress at the reference temperature and reference strain rate (Similar to A value in the case of the JC model),
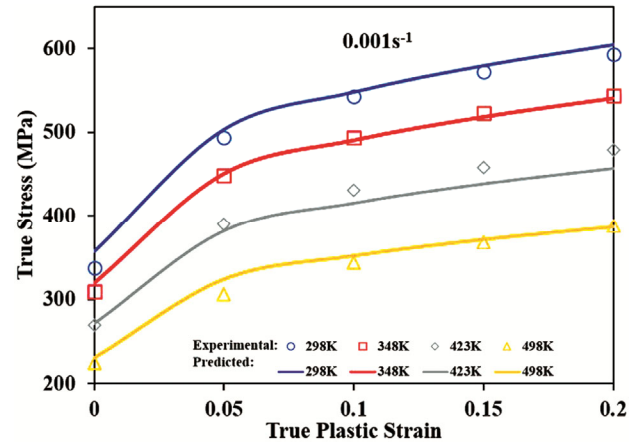


Fig. 2 — Validation of predicted stress with experimental stress data using m-ZA model at 0.001s$^{-1}$ strain rate.
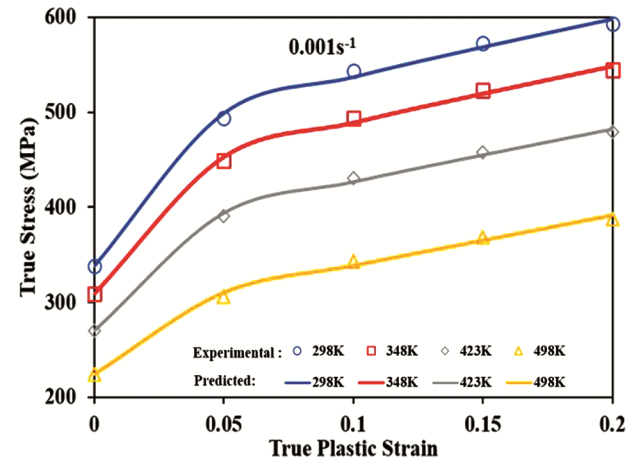


Fig. 3 — Validation of predicted stress with experimental stress data using m-Arr model at 0.001s$^{-1}$strain rate.

$C_2, C_3, C_4, C_5, C_6$ and 'n' are material constants, $\varepsilon$ stands for true plastic strain, $\dot{\varepsilon}^* = \dot{\varepsilon}/\dot{\varepsilon}_0$ is dimensionless strain rate with $\dot{\varepsilon}$ as strain rate and $\dot{\varepsilon}_0$is the reference strain rate,$T^* = T - T_{ref}$ where T is the current temperature, $T_{ref}$ is reference temperature. The $T_{ref}$ is the minimum temperature of the experiments conducted and is equals to 298K. The m-ZA model considers the strain hardening, strain rate hardening, and thermal softening of the material. It also accounts for the coupled effects of temperature – strain hardening and temperature – strain rate hardening. The different material constants of this model are found in the following conditions.

*3.2.1 Condition 1: At reference strain rate*

At reference strain rate, $\dot{\varepsilon} = \dot{\varepsilon}_0 = 0.001s^{-1}$, the $\dot{\varepsilon}^* = 1$. Therefore the Eq. (9) reduces to Eq. (12).

$$\sigma = (C_1 + C_2\varepsilon^n)e^{[-(C_3+C_4\varepsilon)T^*]} \qquad \ldots (12)$$

By taking a natural logarithm on both sides, the Eq. (11) becomes Eq. (13).

$$\ln(\sigma) = \ln(C_1 + C_2\varepsilon^n) - (C_3 + C_4\varepsilon)T^* \qquad \ldots (13)$$

Using the corresponding experimental data (at the reference strain rate of $0.001s^{-1}$, and for each strain value), the plot between $\ln(\sigma)$ vs $T^*$ gives intercept $\ln(C_1 + C_2\varepsilon^n)$ and slope $-(C_3 + C_4\varepsilon)$ for each strain value. Let us say the intercept is $I_1$, the intercept is expressed in Eq. (14).

$$I_1 = \ln(C_1 + C_2\varepsilon^n) \qquad \ldots (14)$$

By taking exponential and natural logarithm on both sides, the Eq. (14) is changed to Eq. (15).

$$\ln(e^{I_1} - C_1) = \ln(C_2) + n \times \ln\varepsilon \qquad \ldots (15)$$

The $C_1$ in Eq. 14 is known from experimental data as the yield stress at reference strain rate and the reference temperature. By plotting graph $\ln(e^{I_1} - C_1)$ vs $\ln\varepsilon$, n is obtained as slope and the $C_2$ can be calculated from the intercept.

Similarly, let us say $S_1$ be the slope obtained from the Eq. (13). The $S_1$ can be expressed as shown in Eq. (16)

$$S_1 = -(C_3 + C_4\varepsilon) \qquad \ldots (16)$$

By plotting the graph between $S_1$ and $\varepsilon$ at reference temperature and reference strain rate, the $C_3$ and $C_4$ values are calculated from intercept and slope, respectively.

### 3.2.2 Condition 2: Consideration of coupled effects

By taking natural logarithm on both sides of Eq. (11), we get

$$\ln(\sigma) = \ln(C_1 + C_2\varepsilon^n) - (C_3 + C_4\varepsilon)T^* + (C_5 + C_6T^*)\ln\dot{\varepsilon}^* \qquad \ldots (17)$$

By plotting graph $\ln(\sigma)$ vs $\ln\dot{\varepsilon}^*$ and say slope of the line is $S_2$ then the slope can be written as in Eq. (18).

$$S_2 = (C_5 + C_6T^*) \qquad \ldots (18)$$

For each temperature and strain, one value of $S_2$ is obtained. Therefore, by plotting the lines $S_2$ vs $T^*$, the $C_6$ and $C_5$ are obtained as slope and intercept respectively. Since there are five sets of these values, the optimization is performed by minimizing the error using Eq. (7) and (8).

All the values of $C_1, C_2, C_3, C_4, C_5, C_6$ and n are shown in Table 2. Using these constants, the Modified Zerilli-Armstrong constitutive equation for the LOS material can be written, as shown in Eq. (19).

$$\sigma = (337.86 + 464.42\varepsilon^{0.3439}) \\ e^{[-(0.0022+0.0002\varepsilon)T^*+(0.001+0.0002T^*)\ln\dot{\varepsilon}^*]} \qquad \ldots (19)$$

The predicted flow stress using the Eq. (19) is compared with the experimental data as it is depicted pictorially in Fig. 2 at three different strain rates of $0.001s^{-1}$, $0.005s^{-1}$, and $0.01s^{-1}$. *Modified-Arrhenius equation(m-Arr)*

Since the modified Arrhenius equation expresses the flow behavior at elevated temperatures and strain rates, several researchers have been using it[24–26]. The Zener-Holloman parameter is a function of temperature and strain rate and it is expressed in Eq. (20).

$$Z = \dot{\varepsilon} \times \exp\left(\frac{Q}{RT}\right) \qquad \ldots (20)$$

Where, $Z$ is Zener-Holloman parameter, $Q$ is activation energy (KJ mol$^{-1}$), $R$ is the universal gas constant (8.314 Jmol$^{-1}$K$^{-1}$), T is the absolute temperature in Kelvin and $\dot{\varepsilon}$ is true plastic strain rate and it is expressed in Eq. (21).

$$\dot{\varepsilon} = A \times F(\sigma) \times \exp\left(\frac{-Q}{RT}\right) \qquad \ldots (21)$$

where A is material constant, and $F(\sigma)$ is expressed in Eq. (22).

$$F(\sigma) = \begin{cases} \sigma^n, \alpha\sigma < 0.8 \\ \exp(\beta\sigma), \alpha\sigma > 1.2 \\ [\sinh(\alpha\sigma)]^n, for\ all\ \sigma \end{cases} \qquad \ldots (22)$$

Where, $\sigma$ is flow stress, $n$, $\beta$ are material constants $\alpha = \beta/n$ and Therefore, by substituting the hyperbolic function $F(\sigma) = [\sinh(\alpha\sigma)]^n$ in Eq. (19), we get an upgraded equation in a hyperbolic sinusoidal form, and it is expressed as in Eq. (23)

$$\dot{\varepsilon} = A \times [\sinh(\alpha\sigma)]^n \times \exp\left(\frac{-Q}{RT}\right) \qquad \ldots (23)$$

Subsequently, by combining Eq.(18) and Eq.(23), the flow stress is expressed in Eq. (24).

$$\sigma = \frac{1}{\alpha}\ln\left\{\left(\frac{Z}{A}\right)^{1/n} + \left[\left(\frac{Z}{A}\right)^{2/n} + 1\right]^{1/2}\right\} \qquad \ldots (24)$$

Table 2 — Constants for modified Zerilli-Armstrong (m-ZA) model

|  | LOS | SRS | TRS |
|---|---|---|---|
| $C_1$(MPa) | 337.86 | 353.75 | 375.26 |
| $C_2$(MPa) | 464.42 | 425.13 | 553.13 |
| $C_3$ | 0.0022 | 0.0023 | 0.0024 |
| $C_4$ | 0.0002 | -0.0016 | -0.0004 |
| $C_5$ | 0.001 | 0.0122 | 0.0113 |
| $C_6$ | 0.0002 | 0.0001 | 0.0003 |
| n | 0.3439 | 0.3943 | 0.5122 |

In the above Eq. (24), the stress is expressed in terms of strain rate and temperature, but the true plastic strain is not included. This Eq. (24) is called the Arrhenius equation. To account for the true plastic strain in Eq. (24), an exponential function has been suggested, and the modified Arrhenius equation is expressed in Eq. (25)

$$\sigma = \frac{\beta_0 \varepsilon^{\beta_1} \exp(-\beta_2 \varepsilon)}{\alpha} \ln \left\{ \left(\frac{Z}{A}\right)^{1/n} + \left[\left(\frac{Z}{A}\right)^{2/n} + 1\right]^{1/2} \right\} \quad \dots (25)$$

Where, $\varepsilon$ referred to as true plastic strain and $\beta_0, \beta_1, \beta_2$ are material constants. In five different conditions, all the materials constants are determined as given below.

### Condition 1: Low-stress levels i.e., at $\alpha\sigma < 0.8$

From Eq. (21) and Eq. (22), at low-stress condition, the strain rate can be expressed as in Eq. (24)

$$\dot{\varepsilon} = A_1 \times \sigma^{n_1} \quad \dots (26)$$

By plotting graph $\ln(\dot{\varepsilon})$ vs $\ln(\sigma)$, $n_1$ is obtained as slope of the line equation.

### Condition 2: High-stress levels i.e., at $\alpha\sigma > 1.2$

At high-stress levels, the strain rate can be expressed from Eq. (21) and Eq. (22) as in Eq. (27).

$$\dot{\varepsilon} = A_2 \times \exp(\beta\sigma) \quad \dots (27)$$

By plotting graph $\ln(\dot{\varepsilon})$ Vs. highest stresses, the $\beta$ yields as the slope of the line.

Since $\beta$ and $n_1$ are determined, the $\alpha$ can be calculated from the Eq. (28).

$$\alpha = \beta/n_1 \quad \dots (28)$$

### Condition 3: If $\alpha$ is known, finding all stresses

Since $\alpha$ is now a known value, one can proceed to the case of all stress levels. By taking logarithm on both sides of Eq. (21), the Eq. (29) is obtained.

$$\ln[\sinh(\alpha\sigma)] = \frac{1}{n}\ln(\dot{\varepsilon}) + \frac{Q}{nRT} - \frac{1}{n}\ln(A) \quad \dots (29)$$

By plotting graph between $\ln[\sinh(\alpha\sigma)]$ and $\ln(\dot{\varepsilon})$, $1/n$ is calculated as the slope from which n

value is obtained. Similarly, by plotting the graph between $\ln[\sinh(\alpha\sigma)]$ and $1/T$, $Q/(nR)$ yields as the slope of the line. The average value of the $Q/(nR)$ is used to calculate $Q$, which is the activation energy of the deformation process.

### Condition 4: If Q is known, finding Z and A values

Since Q value is now known value, the Z values can be calculated from Eq. (18) in which the strain rate and temperature are experimentally fixed values.

Combining the two equations: (20), (21), and taking logarithm on both sides can be expressed as in Eq. (30).

$$\ln(Z) = \ln(A) + n \times \ln[\sinh(\alpha\sigma)] \quad \dots (30)$$

By plotting graph between $\ln(Z)$ and $\ln[\sinh(\alpha\sigma)]$ at a particular strain, the *A* value can be calculated from the intercept of $\ln(A)$.

### Condition 5: Non-linear regression

Now, the material constants $\alpha$, $Q$, $n$ and $A$ values are known (listed in Table 3) and by substituting them in eq. (25) the unknown material constants $\beta_0, \beta_1, \beta_2$ can be found by regression. These values are obtained for each set of temperature and strain rate by non-linear regression. It is performed using the solver perimeter function in an excel sheet, and the values are listed in Tables 4, 5, and 6.

The calculated material constants $\alpha$, $Q$, $n$, $A$, $\beta_0$, $\beta_1$, and $\beta_2$ are used to form the m-Arr equation for LOS, as shown in Eq. (31).

Table 3 — Constants for modified Arrhenius constitutive equation

|  | LOS | SRS | TRS |
|---|---|---|---|
| $n_1$ | 22.693 | 23.4595 | 17.7602 |
| $\beta$ | 0.0386 | 0.0179 | 0.0312 |
| $\alpha$ | 0.0017 | 0.0008 | 0.0017 |
| $n$ | 46.9247 | 54.3239 | 12.7781 |
| $Q$ | 129707.6 | 130937.3 | 36647.55 |
| $A$ | 7.61E+19 | 9.14E+40 | 3490.639 |

Table 4 — $\beta_0$ Values for LOS, SRS, TRS at 0.001s⁻¹, 0.005s⁻¹, and 0.01s⁻¹ strain rates.

| Temperature | 0.001s⁻¹ | | | 0.005 s⁻¹ | | | 0.01 s⁻¹ | | |
|---|---|---|---|---|---|---|---|---|---|
| (K) | LOS | SRS | TRS | LOS | SRS | TRS | LOS | SRS | TRS |
| 298 | 1.111 | 1.038 | 1.098 | 1.162 | 1.15 | 1.132 | 1.177 | 1.232 | 1.178 |
| 348 | 1.139 | 1.09 | 1.158 | 1.205 | 1.204 | 1.185 | 1.233 | 1.193 | 1.138 |
| 423 | 1.137 | 1.111 | 1.19 | 1.175 | 1.061 | 1.049 | 1.175 | 1.21 | 1.156 |
| 498 | 0.947 | 0.922 | 0.997 | 1.047 | 1.019 | 1.014 | 1.009 | 1.102 | 1.058 |

Table 5 — $\beta_1$ Values for LOS, SRS, TRS at 0.001s⁻¹, 0.005s⁻¹, and 0.01s⁻¹ strain rates

| Temperature | 0.001s⁻¹ | | | 0.005 s⁻¹ | | | 0.01 s⁻¹ | | |
|---|---|---|---|---|---|---|---|---|---|
| (K) | LOS | SRS | TRS | LOS | SRS | TRS | LOS | SRS | TRS |
| 298 | 0.057 | 0.039 | 0.039 | 0.058 | 0.039 | 0.039 | 0.052 | 0.048 | 0.048 |
| 348 | 0.055 | 0.041 | 0.041 | 0.061 | 0.051 | 0.051 | 0.061 | 0.047 | 0.047 |
| 423 | 0.053 | 0.047 | 0.047 | 0.053 | 0.03 | 0.03 | 0.049 | 0.046 | 0.046 |
| 498 | 0.042 | 0.038 | 0.038 | 0.044 | 0.036 | 0.036 | 0.042 | 0.042 | 0.042 |

Table 6 — $\beta_2$ Values for LOS, SRS, TRS at 0.001s$^{-1}$, 0.005s$^{-1}$, and 0.01s$^{-1}$ strain rates.

| Temperature | 0.001s$^{-1}$ | | | 0.005 s$^{-1}$ | | | 0.01 s$^{-1}$ | | |
|---|---|---|---|---|---|---|---|---|---|
| (K) | LOS | SRS | TRS | LOS | SRS | TRS | LOS | SRS | TRS |
| 298 | -0.682 | -0.853 | -0.853 | -0.187 | 0.098 | 0.098 | 0.217 | 0.98 | 0.98 |
| 348 | -0.763 | -0.649 | -0.649 | -0.36 | -0.147 | -0.147 | -0.076 | -0.003 | -0.003 |
| 423 | -0.852 | -0.686 | -0.686 | -0.578 | -0.778 | -0.778 | -0.566 | -0.18 | -0.18 |
| 498 | -1.16 | -0.903 | -0.903 | -0.84 | -0.686 | -0.686 | -0.937 | -0.458 | -0.458 |

Table 7 — Comparison of prediction by statistical parameters.

| | Johnson Cook (JC) | | | Modified Zerilli-Armstrong (m-ZA) | | | Modified Arrhenius (m-Arr) | | |
|---|---|---|---|---|---|---|---|---|---|
| | R | $\Delta$(%) | Number of constants | R | $\Delta$(%) | Number of constants | R | $\Delta$(%) | Number of constants |
| LOS | 0.7262 | 11.1421 | 5 | 0.9765 | 4.4640 | 7 | 0.9950 | 1.1132 | 9 |
| SRS | 0.7261 | 12.8346 | 5 | 0.9788 | 4.3042 | 7 | 0.9899 | 1.3215 | 9 |
| TRS | 0.7023 | 12.2308 | 5 | 0.9718 | 4.0847 | 7 | 0.9899 | 1.3215 | 9 |

$$\sigma = \frac{\beta_0 \varepsilon^{\beta_1} \exp(-\beta_2 \varepsilon)}{0.0017} \ln \left\{ \left(\frac{Z}{7.6086e19}\right)^{1/46.9247} + \right.$$

$$\left. \left[\left(\frac{Z}{7.6086e19}\right)^{2/46.9247} + 1\right]^{1/2} \right\} \qquad \ldots (31)$$

Where, $Z = \dot{\varepsilon} \times \exp\left(\frac{129707.63}{8.314 \times T}\right)$.

Using the eq. (31), the stress values are predicted, and also the predicted data is compared with the experimental data, as shown in Fig. 3.

**3.3 Comparison of the constitutive models**

The comparison of constitutive models can be done by considering prediction capability and suitability. The prediction capability has been assessed by the statistical parameters such as correlation coefficient and average absolute error. The usefulness of models has been judged based on the number of constants to be determined. The statistical parameters and number of constants of all three models are listed in Table 7. Fig. 1, Fig. 2, and Fig. 3 illustrate the comparison between experimental and predicted values of the low oxygen sheet Zircaloy – 4 material. As it can be understood from the graphs, the prediction of m-Arr is very close to the experimental values, whereas it is very much deviating in the case of the JC model. It is also evident from Table 7 that the average absolute error is around 11 times lower for the m-Arr compared to that of the JC model.

The Coefficient of correlation, average absolute error, and the number of material constant of the three models corresponding to each material are listed in Table 7. The R values are maximum when the m-Arr model is used to predict the stress. The maximum R values of 0.9950, 0.9899, and 0.9899 are observed in LOS, SRS, and TRS, respectively. The R values are minimal if the JC model is used, and the minimum R values of 0.7262, 0.7261 and 0.7023 are seen in LOS, SRS, and TRS. It is due to the JC model does not

include the coupled effects of strain, strain rate, and temperature together. The Coefficient of correlation values may bias towards higher values or lower values; therefore, to check the proper predictability of the models the average absolute error is considered. The minimum average absolute error among all the three materials is obtained as 1.1132% from the m-Arr, whereas the maximum one is 12.8346% resulted from the JC model. The limitation of the m-Arr is that it requires to determine a greater number of material constants compared to the other two models. In this context, the JC model is fit due to a smaller number of constants to evaluate, but it results in a high average absolute error and less R-value. Even though the m-Arrr equiresa greater number of constants to be evaluated, it results in a very high R-value and less absolute average error among the other two models.

However, the m-Arr and JC constitutive equations come under the phenomenological models. It means they do not consider the physical aspects during the prediction of flow stress. On the other hand, m-ZA is a physical-based model. It considers the physical aspects such as dislocation movements, which activate thermally, thermodynamics theory, slips kinetics, etc. Hence, sometimes, physical-based models are preferred more compared to the phenomenological models. But more important parameters in selecting the constitutive model is high goodness of fit and less absolute average error. Among the three models, the m-Arr has high goodness of fit and less absolute average error.

The discussion considers most aspects, such as statistical parameters, phenomenal and physical aspects, and the number of constants to be evaluated. The results show a very clear indication with the consideration of $R$ and $\Delta$(%) that the m-Arr is very much suitable model for all the three types of zircaloy-4 materials for the prediction of flow stress

even though it has a greater number of constants to be evaluated.

## 4 Conclusion

Three types of zircaloy-4 materials are subjected to tensile tests and tensile flow behavior is modelled. Based on the work, the following conclusions can be made:

- Johnson-Cook model is developed for all the three types of zircaloy-4 materials. It has resulted in very poor goodness of fit with a maximum *R*-value of 0.7262 and a minimum average absolute error of 11.1421% for LOS among the three materials.

- The modified Zerilli-Armstrong model is developed for all three types of zircaloy-4 materials. It has resulted in moderate goodness of fit with a maximum *R*-value of 0.9788 and a delta value of 4.3042% for SRS among the three zircaloy-4 sheet materials.

- Modified Arrhenius type equation is developed for LOS, SRS, and TRS materials. It has resulted in very high goodness of fit with a maximum *R*-value of 0.9950 and a minimum delta value of 1.1132% for LOS material among the three materials.

- The comparison among the three types of constitutive equations shows that the *m-Arr* is suitable for good predictability of flow stress even though it has a greater number of constants to be determined.

## References

1 Limbadri K, Singh S K, Satyanarayana K, Singh A K, Ram A M, Ravindran M, Krishna K V M, Reddy M C, & Suresh K, *Metallogr Microstruct Anal*, 7 (2018) 421.
2 Badrish A, Morchhale A, Kotkunde N, & Singh S K, *Int J Mater Form*, 13 (2020) 445.
3 Qiang Z, Wen C, Jun L, Shuhai H, & Xiangsheng X, *Int J Mater Form*, 13 (2020) 293.
4 Saxena A, Kumaraswamy A, Kotkunde N, & Suresh K, *J Mater Eng Perform*, 28 (2019) 6505.
5 Su N, Chen M, Zhang W, Xie L, & Tang W, *J Mater Eng Perform*, 29 (2020) 1194.
6 Rudra A, Das S, & Dasgupta R. *J Mater Eng Perform*, 28 (2019) 87.
7 Kotkunde N, Deole A D, Gupta A K, & Singh S K, *Mater Des*, 55 (2014) 999.
8 Tao Z, Fan X, Yang H, Ma J, & Li H, *Trans Nonferrous Met Soc China*, 28 (2018) 298.
9 Zhang L, Pellegrino A, & Petrinic N, *Def Technol*, 1507 (2020) 032047.
10 Geng P, Qin G, Zhou J, & Zou Z, *J Manuf Process*, 32 (2018) 469.
11 Zhang H, Chen G, Chen Q, Han F, & Zhao Z, *J Alloys Compd*, 743 (2018) 283.
12 Bodunrin M O, *J Mater Res Technol*, 9 (2020) 2376.
13 Gupta A K, Anirudh V K, & Singh S K, *Mater Des*, 43 (2013) 410.
14 Chakravarthi KVA, Koundinya NTBN, Murty SVSN, & Rao BN, *Def Technol*, 14 (2018) 51.
15 Wang X D, Pan Q L, Xiong S W, Liu L L, Sun Y W, & Wang W Y, *Trans Nonferrous Met Soc China (English Ed.)*, 28 (2018) 1484.
16 Che J, Zhou T, Liang Z, Wu J, & Wang X, *J Brazilian Soc Mech Sci Eng*, (2018) 40.
17 Lin Y, Zhang K, He Z, Fan X, Yan Y, & Yuan S, *J Mater Eng Perform*, 27 (2018) 2475.
18 Rasaee S, Mirzaei A H, & Almasi D, *Bull Mater Sci*, (2020) 43.
19 Deng S, Song H, Zheng C, Zhang S, & Chu L, *Int J Mater Form*, 12 (2019) 321.
20 Le Saux M, Besson J, Carassou S, Poussard C, & Averty X, *J Nucl Mater*, 378 (2008) 60.
21 Le Saux M, Besson J, & Carassou S *J, Nucl Mater*, 446 (2015) 43.
22 Rickhey F, Kim M, Lee H, & Kim N, *Mater Des*, 65 (2015) 995.
23 Gupta A K, Krishnamurthy H N, Singh Y, Prasad K M, & Singh S K, *Mater Des*, 45 (2013) 616.
24 Liu L, Xin W Y, Gong H, & Wang K, *Trans Nonferrous Met Soc China* (*English Ed.*), 29 (2019) 448.
25 Chen F, Zhao X, Ren J, Chen H, & Zhang X, *Met Mater Int*, 27 (2019) 1728.
26 Wei D, Liu R, Zuo C, & Zhou H, *Met Mater Int*, 26 (2020) 739.